Na+ Current in Human Atrial Myofibroblasts Alters Myocyte Excitability: A Computational Study

Heqing Zhan[1], Jialun Lin[1], Xiaoling Li[1], Jingtao Zhang[2]

[1] Department of Information Technology, Hainan Medical University, Haikou, 571199, China
[2] Cardiac Arrhythmia Center, Fuwai Hospital, National Center for Cardiovascular Diseases, Beijing, 100037, China

Abstract

Previous studies have shown that human atrial myofibroblasts can express a Na+ current (I_{Na_myofb}). This preliminary study aimed to identify the role of I_{Na_myofb} integrated in electrotonic myofibroblast-myocyte (myofb-m) coupling on the excitability and repolarization of myocyte and myofibroblast. Mathematical modeling was done using a combination of (1) the Maleckar et al. model of the human atrial myocyte, (2) the MacCannell et al. "active" model of the human cardiac myofibroblast, and (3) our formulation of I_{Na_myofb} based upon experimental findings from Chatelier et al. The results showed that (1) for myocytes, the addition of I_{Na_myofb} decreased the reductions of the peak of action potential (V_{max}) and action potential duration (APD), and increased the degree of resting membrane potential (V_{rest}) depolarization as compared to no I_{Na_myofb} integrated in myofb-m coupling. (2) for myofibroblasts, more significant electrotonic depolarizations were exhibited with addition of I_{Na_myofb}. I_{Na_myofb} should be considered in future pathological cardiac mathematical modeling, such as atrial fibrillation and cardiac fibrosis.

1. Introduction

Fibroblasts, which represent the most abundant cell type in cardiac tissue, are now accepted as key contributors to development, adaptation, and disease-related remodeling of the heart. In pathological conditions, such as atrial fibrillation and heart failure, fibroblasts proliferate, migrate and differentiate into myofibroblasts and lead to cardiac fibrosis [1]. Since gap junction proteins and voltage gated ion channels have been identified in fibroblasts and myofibroblasts, these cells have not been considered as non-excitable cells. They were proposed to function as a current source and sink when coupled to myocytes [2, 3].

Recent computational studies have investigated effects of electrotonic myofb-m coupling on the excitability and repolarization of myocyte and myofibroblast. Their simulation results revealed that myofb-m coupling reduced V_{max}, shortened APD and depolarized V_{rest} in myocytes [4, 5].

Since fibroblasts and myofibroblasts are involved in cardiac pathological processes, it is necessary to confirm ionic channel expression in these cells. Several K+ channels and non-selective cationic channels have been identified and been integrated in simulations of myofibroblast [3, 6]. Moreover, it has been reported that myofibroblasts isolated from human atrial tissue expressed Na+ current and this current was generated by Na_v 1.5 α subunit [7].

In this study, the mathematical formulation of I_{Na_myofb} was developed on the base of previous experimental findings [7], and then I_{Na_myofb} was integrated with the MacCannell et al. "active" model of the human cardiac myofibroblast and the Maleckar et al. model of the human atrial myocyte [6, 8]. The number of coupled myofibroblasts and values of intercellular resistance were selected to investigate the effects of I_{Na_myofb} on the excitability and repolarization of myocyte and myofibroblast in this cell-cell interaction.

2. Materials and methods

2.1. Myofb-m coupling

According to [6], the differential equation for the membrane potential of the cell was given by

$$C\frac{dV}{dt} = -I_{\text{ion}} + \sum_{k=1}^{n} G_{\text{gap}}(V^k - V), \qquad (1)$$

where C is the membrane capacitance of the myocyte or myofibroblast, I_{ion} and V represent the transmembrane current and potential of the myocyte or myofibroblast, respectively, n is the number of coupled myofibroblasts, and G_{gap} is the intercellular myofb-m conductance. In these simulations, one and eight myofibroblasts were coupled to a single myocyte by assigning a G_{gap} which varied between 0.5 and 8 nS in individual simulations.

2.2. Model of the human atrial myocyte

The Maleckar et al. model of the human atrial myocyte was used for its computationally efficient and internally consistent [8].

2.3. Model of human atrial myofibroblasts

The "active" electrophysiological model of the human atrial myofibroblast was based on the general formulation of MacCannell et al. [6]. According to the experimentally recorded values of myofibroblasts, V_{rest} and the membrane capacitance were chosen to be -47.8 mV and 6.3 pF, respectively [9].

In order to identify the role of I_{Na_myofb} on myocyte and myofibroblast excitability, a mathematical formulation was based upon experimental results from Chatelier et al. [7]. They provided evidence that I_{Na_myofb} was generated by the same Na_v 1.5 which produced Na^+ currents in the atria and ventricles of the adult human heart [7]. Therefore, the equation of Luo and Rudy for the fast Na^+ current was applied and modified here to simulate I_{Na_myofb} [10]. The formulation was as follows,

$$I_{Na\_myofb} = g_{Na} \times m_{Na} \times j_{Na}^{0.12} \times (V_{myofb} - E_{Na}), \qquad (2)$$

where g_{Na}, the maximum conductance of I_{Na_myofb}, was 0.04 nS/pF. E_{Na} was the Nernst potential for Na^+ ions. m_{Na} and j_{Na} were the activation and inactivation parameters, respectively. In order to conform to the experiment data [7], j was made to be $j^{0.12}$. The time dependence was given by

$$\frac{dm_{Na}}{dt} = \frac{m_{Na} - \overline{m}}{\tau_m} \qquad (3)$$

and

$$\frac{dj_{Na}}{dt} = \frac{j_{Na} - \overline{j}}{\tau_j}. \qquad (4)$$

The steady-state activation and inactivation parameters were given by

$$\overline{m} = \frac{-0.0102 - 1.0063}{1.0 + \exp((V_{myofb} + 42.10)/10.53)} + 1.0063 \qquad (5)$$

and

$$\overline{j} = \frac{1.04 - 0.004}{1.0 + \exp((V_{myofb} + 84.82)/9.40)} + 0.004. \qquad (6)$$

The functions describing τ_m and τ_j were given by

$$\alpha_m = \begin{cases} 0.0077 \dfrac{V_{myofb} + 68.19}{1 - \exp(-0.18(V_{myofb} + 68.19))} \\ 0.0433, \quad \text{if } V_{myofb} = -68.19 \end{cases} \qquad (7)$$

$$\beta_m = 0.004 \exp\left(-\frac{V_{myofb}}{11.98}\right) \qquad (8)$$

$$\alpha_j = \begin{cases} \left[-14.5\exp(0.17V_{myofb}) + 1.8\exp(1.56V_{myofb})\right] \times \\ \dfrac{V_{myofb} + 35.73}{1 + \exp\left[3.31(V_{myofb} + 3.86)\right]} \\ 0, \quad \text{if } V_{myofb} \geq -40 \end{cases} \qquad (9)$$

$$\beta_j = \begin{cases} 5.05 \times 10^{-5} \dfrac{\exp(-0.0995V_{myofb})}{1 + \exp\left[-0.01(V_{myofb} - 84.02)\right]} \\ 0.11 \dfrac{\exp(-4.13 \times 10^{-4}V_{myofb})}{1 + \exp\left[-0.09(V_{myofb} + 42.44)\right]}, \quad \text{if } V_{myofb} \geq -40 \end{cases} \qquad (10)$$

$$\tau_\phi = (\alpha_\phi + \beta_\phi)^{-1}, \quad \text{for } \phi = m, j \qquad (11)$$

where α_ϕ and β_ϕ were the extrapolated rate coefficients.

2.4. Simulation protocol and numerical methods

Simulations were carried out with one active myofibroblast coupled to a single atrial myocyte in which G_{gap} was varied between 0.5 and 8 nS, or with one and eight identical active myofibroblasts coupled to a single atrial myocyte at a constant G_{gap} of 0.5 nS. To ensure that the coupled system reached steady state, 100 stimuli were applied before recording the values of the coupled cells. All state variables were updated by means of the forward Euler method. The time step was set to be 10 μs to ensure numerical accuracy and stability.

3. Results

3.1. Na^+ current in myofibroblasts

Figure 1 shows the steady state activation and inactivation curves, time constants, as well as the peak current-voltage (*I-V*) relationship of I_{Na_myofb}. All curves are consistent with the experimental data from Chatelier et al. [7].

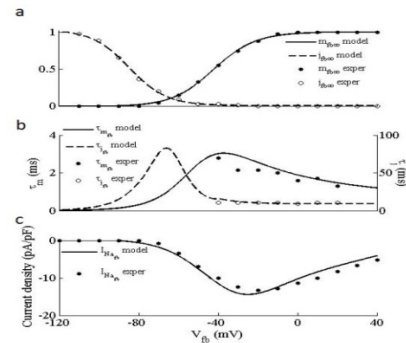
Figure 1. Model representation of parameters describing I_{Na_myofb}. (a) Steady state activation (solid line) and inactivation (dash line) curves, (b) gating variable fast (solid line) and slow (dash line) time constants, (c) *I-V* relationship (solid line). Experimental data (filled and open circles) from Chatelier et al.

are included for comparison.

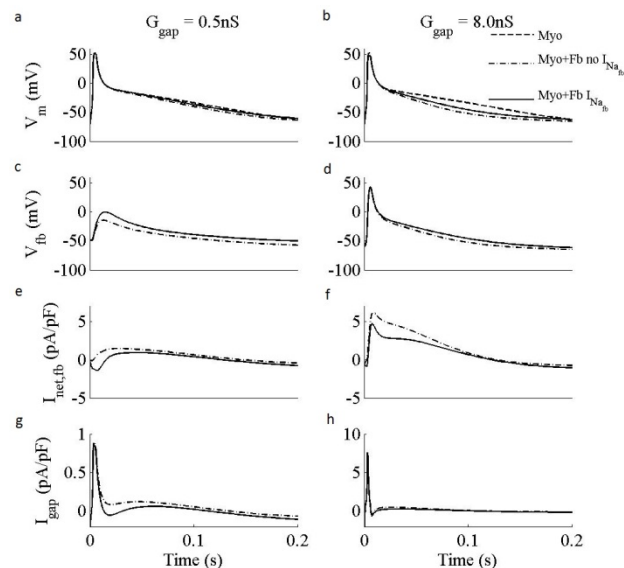## 3.2. Effects of I_{Na_myofb} on myocyte and myofibroblast

Figure 2. Illustration of changes in the waveform of (a,b) the myocyte action potential, (c,d) myofibroblast membrane potential, (e,f) myofibroblast net transmembrane current, and (g,h) gap junction current, during an atrial action potential with only myocyte (dash line), myofb-m coupling without I_{Na_myofb} (chain line) or myofb-m coupling with I_{Na_myofb} (solid line), by coupling one active myofibroblast to an atrial myocyte with a G_{gap} of 0.5 and 8 nS.

Figure 2 shows the effects of I_{Na_myofb} on the membrane potential and current of both cells by coupling one active myofibroblast to an atrial myocyte with a G_{gap} of 0.5 and 8 nS. Whether or not I_{Na_myofb} was integrated in the myofibroblast, myofb-m coupling with either G_{gap} resulted in the reduction of V_{max} and APD and the depolarization of V_{rest} in the myocyte, as well as the depolarization in the myofibroblast. However, after addition of I_{Na_myofb}, the reduction of V_{max} and APD in the myocyte has decreased, and the degree of V_{rest} depolarization has increased (Figure 2a and 2b). For example, with G_{gap} of 8 nS, V_{max} was decreased by 8.7% (myofb-m coupling without I_{Na_myofb}) and 8.4% (myofb-m coupling with I_{Na_myofb}) in comparison with the control (only myocyte). APD (90% repolarization) was decreased by 21.4% and 2.7%, respectively. V_{rest} was increased by 3.8% and 5.6%, respectively. For myofibroblasts, more significant electrotonic depolarizations were exhibited with addition of I_{Na_myofb} (Figure 2c and 2d). For example, with G_{gap} of 0.5 nS, V_{max} of the myofibroblast was -14.3 mV (without I_{Na_myofb}) and -0.1 mV (with I_{Na_myofb}), respectively (a 14.1% increase). V_{rest} of the myofibroblast was -61.6 mV (without I_{Na_myofb}) and -52.3 mV (with I_{Na_myofb}), respectively (a 15.2% increase). Figure 2e and

2f demonstrated that integrating I_{Na_myofb} in the myofibroblast resulted in the reduction of the net transmembrane current in the collective myofibroblast population ($I_{net,fb}$). Figure 2g and 2f illustrated that the current flowing through the intercellular gap junctions (I_{gap}) has fallen slightly with addition of I_{Na_myofb}.
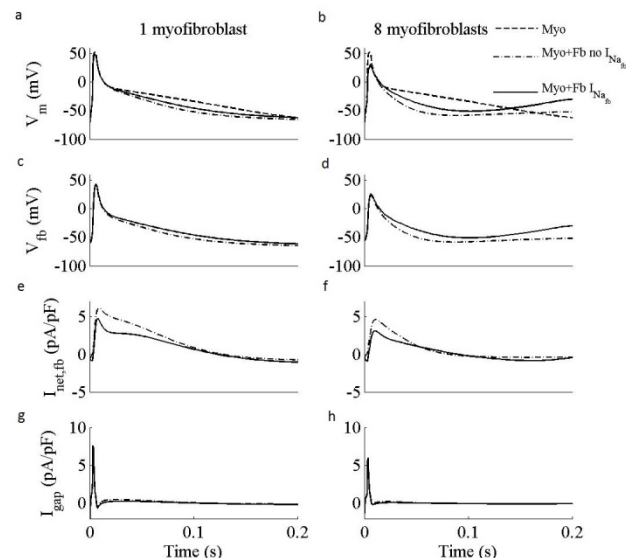

Figure 3. Illustration of changes in the waveform of (a,b) the myocyte action potential, (c,d) myofibroblast membrane potential, (e,f) myofibroblast net transmembrane current, and (g,h) gap junction current, during a atrial action potential with only myocyte (dash line), coupling without I_{Na_myofb} (chain line) or coupling with I_{Na_myofb} (solid line), by coupling one and eight active myofibroblasts to an atrial myocyte with a G_{gap} of 8 nS.

Figure 3 shows similar effects of I_{Na_myofb} on the membrane potential and current of both cells when G_{gap} is fixed at 8 nS and the number of coupled myofibroblasts is 1 and 8. Integrating I_{Na_myofb} into the myofibroblast resulted in smaller reduction in V_{max} and APD for the myocyte, and greater depolarization in V_{rest} for both cells. $I_{net,fb}$ and I_{gap} have fallen down in comparison with the situation of myofb-m coupling without I_{Na_myofb}. When the number of coupled myofibroblasts became greater, the above effects were more significant.

4. Discussion

In this study, we developed a mathematical formulation of I_{Na_myofb} and integrated it into the active myofibroblast model. The simulations provide novel insights into the roles of I_{Na_myofb} on the excitability and repolarization of myocyte and myofibroblast.

Chatelier et al. used a double exponential function to fit the time courses of current decay elicited at depolarized voltages [7]. Here, we used a multiple parameter exponential function modeled after the equation of time courses by Luo and Rudy [10] because

of the evidence that electrophysiological properties of $I_{\text{Na\_myofb}}$ were similar to those of sodium channels found in cardiac myocytes [7, 11].

Comparing to the results from Koivumaki et al. [12], our simulations have shown significant effects of $I_{\text{Na\_myofb}}$ on the excitability and repolarization of myocyte and myofibroblast. Unlike the reasoning that $I_{\text{Na\_myofb}}$ might be inactive when V_{rest} of myofibroblasts was -35 or -65 mV [12], $I_{\text{Na\_myofb}}$ in our simulation was activated during an atrial action potential. Moreover, the effects that $I_{\text{Na\_myofb}}$ decreased the reductions of V_{max} and APD and increased the degree of V_{rest} depolarization in myocytes would be expected to change diastolic Ca^{2+} levels and conduction velocity.

A major limitation of the mathematical modeling is that, the influence of homologous coupling between adjacent myofibroblasts is not considered. Because myofibroblasts can form conduction bridges between myocyte bundles and introduce nonlinearity into the coupled model to alter the electrophysiological properties of the coupled myocyte, coupling between myofibroblasts may be important in tissue modeling [8, 13]. Besides, the influence of stretch activated ionic channels in myocytes and myofibroblasts is not considered, which can alter cardiac electrical activity by the mechanoelectric feedback [14].

5.   Summary

In conclusion, the formulation of $I_{\text{Na\_myofb}}$ has been developed and integrated in myofb-m coupling. The simulation results suggest that the addition of $I_{\text{Na\_myofb}}$ decrease the reductions of V_{max} and APD and increase the degree of V_{rest} depolarization in myocyte, and exhibit more significant electrotonic depolarizations in myofibroblasts. The effect proves that $I_{\text{Na\_myofb}}$ should be considered in future pathological cardiac mathematical modeling, such as atrial fibrillation and cardiac fibrosis.

Acknowledgements

References

[1]   Segura A M, O H Frazier, and L M Buja. Fibrosis and heart failure. Heart Fail Rev, 2014; 19(2): 173-85.
[2]   Shibukawa Y, E L Chilton, K A Maccannell, R B Clark, and W R Giles. K+ currents activated by depolarization in cardiac fibroblasts. Biophys J, 2005; 88(6): 3924-35.
[3]   McDowell K S, F Vadakkumpadan, R Blake, J Blauer, G Plank, R S Macleod, and N A Trayanova. Mechanistic inquiry into the role of tissue remodeling in fibrotic lesions in human atrial fibrillation. Biophys J, 2013; 104(12): 2764-73.
[4]   Ashihara T, R Haraguchi, K Nakazawa, T Namba, T Ikeda, Y Nakazawa, T Ozawa, M Ito, M Horie, and N A Trayanova. The role of fibroblasts in complex fractionated electrograms during persistent/permanent atrial fibrillation: implications for electrogram-based catheter ablation. Circulation Research, 2012; 110(2): 275-84.
[5]   Aguilar M, X Y Qi, H Huang, and S Nattel. Fibroblast electrical remodeling in heart failure and potential effects on atrial fibrillation. Biophys J, 2014; 107(10): 2444-55.
[6]   MacCannell K A, H Bazzazi, L Chilton, Y Shibukawa, R B Clark, and W R Giles. A mathematical model of electrotonic interactions between ventricular myocytes and fibroblasts. Biophysical Journal, 2007; 92(11): 4121-4132.
[7]   Chatelier A, A Mercier, B Tremblier, O Theriault, M Moubarak, N Benamer, P Corbi, P Bois, M Chahine, and J F Faivre. A distinct de novo expression of Nav1.5 sodium channels in human atrial fibroblasts differentiated into myofibroblasts. J Physiol, 2012; 590(17): 4307-19.
[8]   Maleckar M M, J L Greenstein, W R Giles, and N A Trayanova. K+ current changes account for the rate dependence of the action potential in the human atrial myocyte. Am J Physiol Heart Circ Physiol, 2009; 297(4): H1398-410.
[9]   Chilton L, S Ohya, D Freed, E George, V Drobic, Y Shibukawa, K A Maccannell, Y Imaizumi, R B Clark, I M Dixon, and W R Giles. K+ currents regulate the resting membrane potential, proliferation, and contractile responses in ventricular fibroblasts and myofibroblasts. Am J Physiol Heart Circ Physiol, 2005; 288(6): H2931-9.
[10]   Luo C H and Y Rudy. A dynamic model of the cardiac ventricular action potential. I. Simulations of ionic currents and concentration changes. Circulation Research, 1994; 74(6): 1071-96.
[11]   Li G R, H Y Sun, X H Zhang, L C Cheng, S W Chiu, H F Tse, and C P Lau. Omega-3 polyunsaturated fatty acids inhibit transient outward and ultra-rapid delayed rectifier K+currents and Na+current in human atrial myocytes. Cardiovasc Res, 2009; 81(2): 286-93.
[12]   Koivumaki J T, R B Clark, D Belke, C Kondo, P W Fedak, M M Maleckar, and W R Giles. Na(+) current expression in human atrial myofibroblasts: identity and functional roles. Front Physiol, 2014; 5: 275.
[13]   Miragoli M, G Gaudesius, and S Rohr. Electrotonic modulation of cardiac impulse conduction by myofibroblasts. Circulation Research, 2006; 98(6): 801-810.
[14]   Sassoli C, F Chellini, R Squecco, A Tani, E Idrizaj, D Nosi, M Giannelli, and S Zecchi-Orlandini. Low intensity 635 nm diode laser irradiation inhibits fibroblast–myofibroblast transition reducing TRPC1 channel expression/activity: New perspectives for tissue fibrosis treatment. Lasers in Surgery and Medicine, 2016; 48(3): 318-332.

Address for correspondence.

Heqing Zhan
Department of Information Technology, Hainan Medical University, Haikou, 571199, China
E-mail: zhq86zijing@163.com